MODEL FOR CONCRETE CONFINED BY ARAMID FRP

Chris BURGOYNE [1] Hau-Yan LEUNG [2]

[1] Department of Engineering, University of Cambridge, UK
[2] School of Construction, Unitec, Auckland, New Zealand

Keywords: aramid, compression, confinement, analysis

1 INTRODUCTION

The advent of Fibre Reinforced Plastic (FRP) as reinforcement or as prestressing tendons for concrete has many attractions, since they are more durable than steel. However, they show no ductility before failure (although their large strain capacity normally means they are unlikely to snap), which means that beams will normally be designed to be over-reinforced. Thus, instead of failure being initiated by yielding of the steel, with the concrete failing later, it will be caused by crushing of the concrete. Hitherto it has been enough to say that the concrete has *sufficient* strength, without requiring too much understanding of the actual failure process, but if the concrete is going to fail first more detail is required.

It is also desirable for the concrete to have greater ductility, and to this end, it has been suggested [1] that spirals of reinforcement should be included in the compression zone (with their axes aligned parallel to the compressive force) to provide additional confinement; if FRPs are being used as the tension reinforcement it is logical to use them also for the hoop reinforcement. Although rectangular links can be made from steel, they are not ideal for FRP because of strength loss in the corners, and they are anyway less efficient at generating confining stress than circular links.

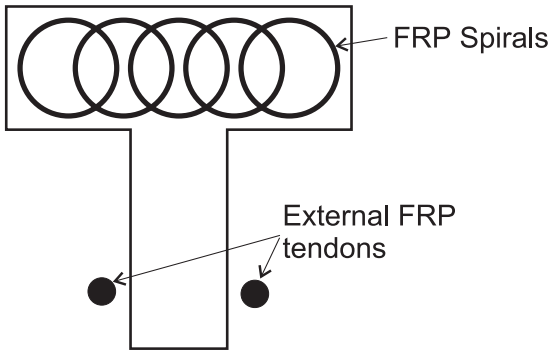

Fig. 1 Novel beam design.

The applications envisaged are in beams, where it makes both structural and practical sense for them to have rectangular compression flanges (Figure 1). Thus, to maximise the area that is to be confined, it is possible to envisage a rectangular compression flange that contains a series of overlapping spirals. There will thus be three types of concrete to be considered – the unconfined concrete in the cover region, the singly-confined concrete inside one spiral, and doubly-confined concrete in the regions where two spirals overlap. There have been many studies where researchers have conducted tests on confined concrete, to which curves have been fitted, but very little work that goes back to the fundamental properties of concrete in such a way that the important factors can be investigated. This paper proposes such an analytical model for both types of confined concrete. Space does not permit here the comparisons that have been carried out with tests, but these have been done and are reported elsewhere. The model here has been extended to determine the moment-curvature relationship for beams, which have also been tested experimentally [2].

Many tests [3-9] have shown that unconfined plain concrete, in particular high strength concrete, exhibits a brittle failure mode; the failure may be explosive and marks the termination of the stress-strain curve and loss of load-carrying capacity shortly after the peak load. Under deformation control, the stress-strain curve normally includes a monotonically increasing branch up to a peak value, followed by a descending part that gradually flattens to a constant value. The initial portion of the

ascending branch is linearly elastic but at about 70% of the ultimate strength, the presence of microcracks leads to non-linear behaviour, with a reduction in tangent modulus. In the subsequent descending branch the concrete is severely damaged with prominent cracks. There is a small lateral expansion during the ascending phase, associated with normal Poisson's ratio effects and an increase in volume caused by the microcracks, but the lateral expansion increases dramatically after the peak as the cracks expand.

However, if there exists a lateral pressure which resists this sideways expansion, the core concrete will be in a state of multi-axial compression; both the deformation capacity and strength are improved [10-17]. There are two means of confinement to provide the lateral pressure, *active* and *passive*. Both aim to restrict the core concrete from expansion but the mechanism used to induce the confining pressure is different.

In active confinement, the lateral pressure is applied by an external force whose value is known or can even be controlled in response to the applied load. Kotsovos has presented the results of a study of concrete loaded in this way, which can be used to determine the relevant load-extension curves [10]. It does not, however, represent the behaviour of concrete where the confining stress comes from reinforcement inside, or on the surface of, the concrete.

Passive confinement arises when the lateral expansion of the concrete is resisted by confining reinforcement; the confining pressure is highly dependant upon the relationship between axial applied stress and the induced lateral strain. The concrete bears the axial load because of the stress state induced by the lateral reinforcement. In the ascending part of the stress-strain curve the confining effect is small since the lateral expansion is small, but the descending portion of the stress-strain response is dominated by the behaviour of the confining reinforcement that resists the lateral expansion, establishing a multi-axial state of stress in the core concrete.

2 ACTIVELY-CONFINED CONCRETE

The analysis presented here is based on Kotsovos' study of concrete subjected to active hydraulic pressure [6]. He recognised that most concrete structural members are subjected to a multi-axial stress state. Kotsovos and Newman made a mathematical prediction of the stress-strain response of concrete in terms of the hydrostatic (σ_o) and deviatoric (τ_o) stress invariants [18,19]. They performed an extensive experimental study to obtain the stress-strain profile of concrete cylinders subjected to different hydraulic pressures, and proposed empirical equations. Crack extension was identified as the main cause of fracture; deviatoric stress tends to give a uni-directional fracture in the direction of maximum compressive stress, while hydrostatic stress gives random crack propagation that reduces the rate of fracture caused by the deviatoric stress. Since any state of stress can be decomposed into hydrostatic and deviatoric stresses, the behaviour of concrete under a generalised stress condition can be defined by using these components. The work was later extended [6] by introducing the concept of an internal stress σ_{id} which allows a deviatoric stress to generate a hydrostatic strain $\varepsilon_{o(d)}$.

By using Kotsovos' model, the complete stress-strain profile for actively-confined concrete subjected to any combination of constant lateral pressures can be obtained. The model assumes that the axial stress is the major principal stress σ_1, and the lateral confining stresses σ_2 and σ_3 are known (or can be assumed). The model then gives the variation of the corresponding strains as the axial load changes. Full details of the equations that underlie the method are given elsewhere [20]; the procedures can be summarised as follows:

1. The values of the lateral confining stresses σ_2 and σ_3 are fixed.
2. The value of the axial stress σ_1 that corresponds to the ultimate state is calculated.
3. The ascending portions of the axial stress-axial strain and axial stress-lateral strain curves are calculated.
4. For the post-ultimate state, the variation of the stress state $\delta\sigma_i$ and strain state $\delta\varepsilon_i$ (i=1,2,3) can then be found.

This formulation is applicable to concrete subjected to constant (active) confining pressure. However, when concrete is surrounded by reinforcement, it is subjected to a passive confining pressure; the established model is not adequate since the confining pressures are not known.

3 PASSIVE CONFINEMENT WITH A SINGLE SPIRAL

When spiral reinforcement is used to provide lateral pressure to the concrete, the confining pressure varies throughout the course of loading and is dependant on the radial strain.

Consider a circular concrete cylinder reinforced with a single spiral whose properties are known. Symmetry requires that $\sigma_2 = \sigma_3 = \sigma_L$; final failure is expected when the spiral snaps which is not usually at the peak load. The analysis can be performed in the following steps, which are shown diagrammatically in Figure 2.

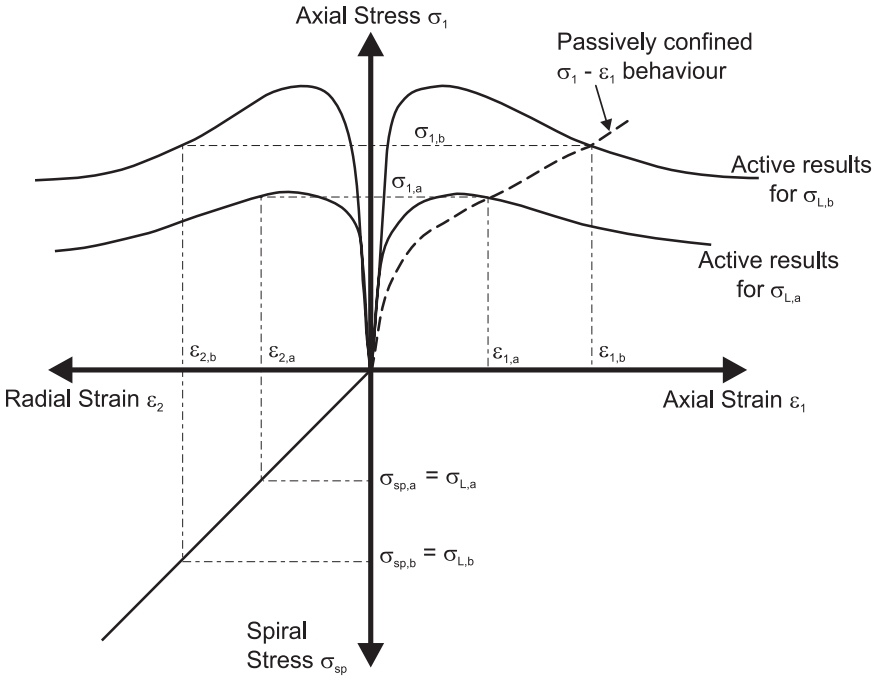

Fig. 2 Model for passive FRP confinement.

1. Compatibility between the transverse concrete strain, ε_2, and the strain of the confining spiral reinforcement, ε_{sp}, is assumed, so $\varepsilon_2 = \varepsilon_{sp}$. The breaking strain of the spiral (ε_{sp}^u) then defines the ultimate lateral strain (ε_2^u).
2. The relationship between the tensile stress in the spiral, σ_{sp}, and the spiral strain, ε_{sp}, is known:

$$\sigma_{sp} = E_{sp}\varepsilon_{sp} = E_{sp}\varepsilon_2 \qquad 0 \le \varepsilon_2 \le \varepsilon_2^u \tag{1}$$

   where E_{sp} denotes the elastic modulus of the spiral.
3. The equivalent active confining stress $\sigma_L (= \sigma_2 = \sigma_3)$, is then calculated by:

$$\sigma_L = \frac{2A_{sp}}{d_c s}\left(1 - \frac{s}{d_c}\right)E_{sp}\varepsilon_2 \tag{2}$$

   where A_{sp} is the cross section area of spiral, d_c is the diameter of confined concrete, and s is the spiral spacing; the term $(1 - s/d_c)$ reduces the confining effect as the spiral pitch increases and implicitly assumes that $s < d_c$.
4. The σ_1-ε_2 and σ_1-ε_1 curves are generated for the calculated σ_L using Kotsovos' active model, as described in Section 2 above. The axial stress σ_1 that generates the assumed value of ε_2 is then determined from the σ_1-ε_2 curve.
5. The corresponding value of ε_1 can then be found from the σ_1-ε_1 curve. This represents one point on the passive stress-strain response of the specimen.

6. By repeating the procedures (2) to (5) for a range of values of ε_{sp} from 0 to ε_{sp}^{u}, the complete σ_1 - ε_1 profile for the passively confined concrete cylinder can be established.

The procedure is slightly modified when steel reinforcement is used, as illustrated in Figure 3. The confining stress reaches a limiting value (at σ_L^*) when the steel reaches its yield point, but it continues to sustain a load as the steel yields with the confining stress remaining effectively constant. The stress-strain curve of the steel-confined concrete then follows the active $\sigma_1 - \varepsilon_1$ curve for σ_L^*.

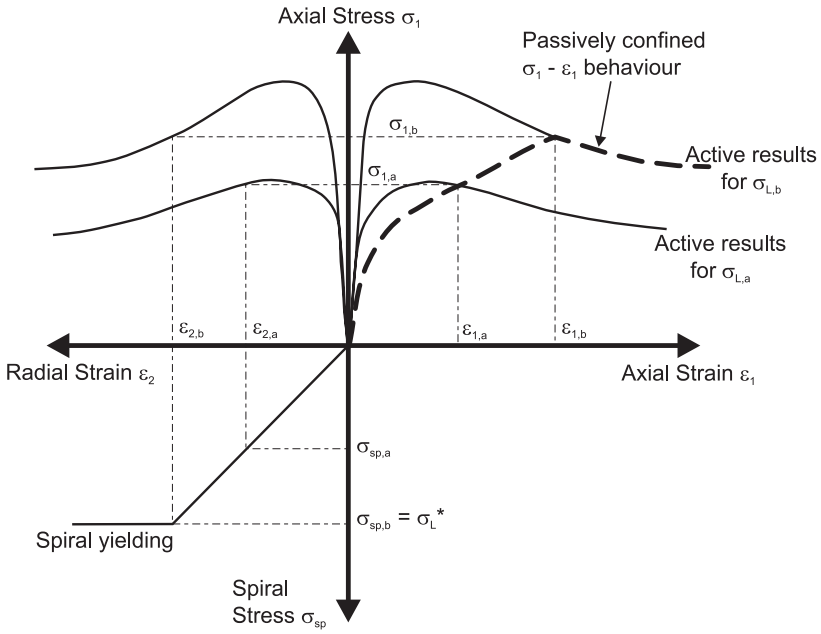

Fig. 3 Model for passive steel confinement.

3.1 Results for passively confined concrete

All the results presented below are for a circular cylinder confined within a spiral of aramid reinforcement [2]. The diameter of the spiral is 90 mm, with a cross-sectional area of 5.3 mm^2. The effective strength of the spiral is 456 MPa at a strain of 1.53%. The uniaxial cylinder strength of the concrete is varied, as is the spiral spacing.

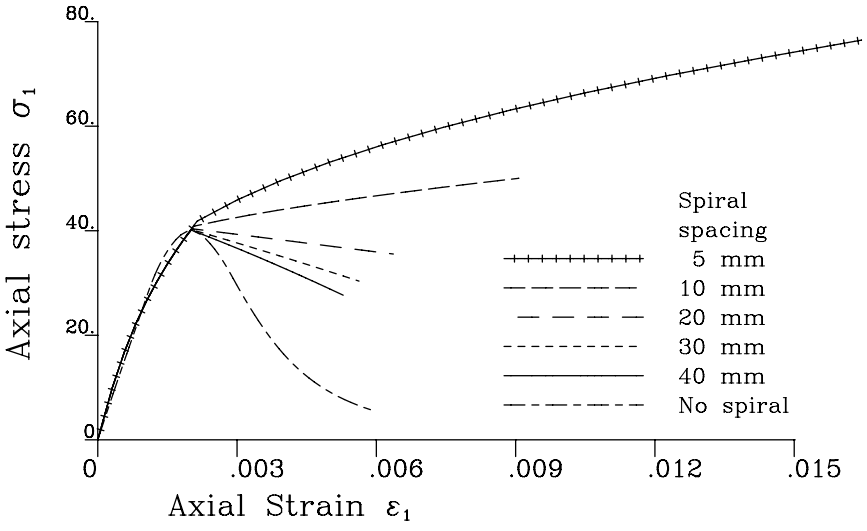

Fig. 4 Effect of varying spiral spacing - (f_c= 40 MPa, aramid spirals).

The effect of varying the spiral pitch is shown in Figure 4 for concrete with a strength of 40 MPa. Reducing the spiral pitch increases the strain capacity of the concrete; for *s* below about 15 mm the concrete gains strength and significant enhancement of capacity is predicted for spacings of 5 mm. Also shown on the figure is the $\sigma_1 - \varepsilon_1$ response for unconfined concrete as predicted by Carreira and Chu [21]. It can be seen that the confining reinforcement has very little effect until internal fracture starts to occur in the concrete with a corresponding increase in specimen volume.

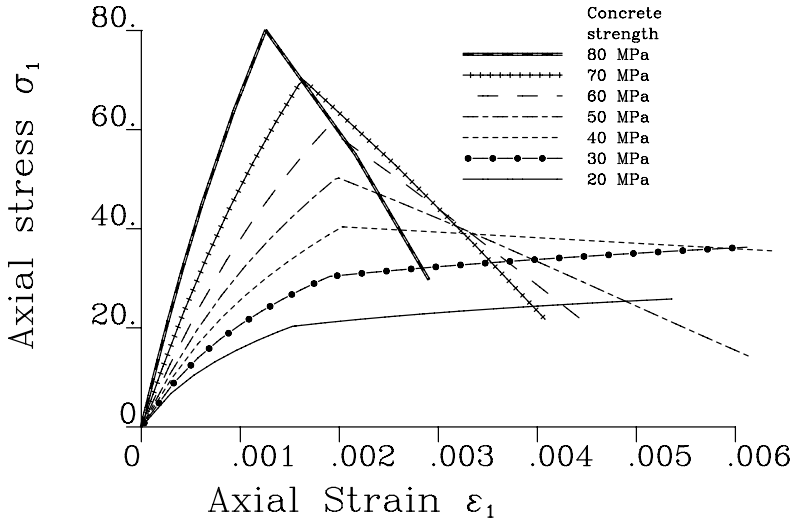

Fig. 5 Effect of varying concrete strength - (aramid spirals, spacing = 20 mm).

The effect of varying concrete strength is shown in Figure 5. The spiral spacing is held constant at 20 mm, but the concrete strength is varied from 20 MPa to 80 MPa. (It should be noted here that Kotsovos' equations are only calibrated up to 65 MPa). As expected the stiffness increases as the concrete gets stronger, but the beneficial effects of the confinement are reduced; stiffer concrete produces less lateral expansion, so the confining stress is reduced in real terms, and even more so as a proportion of the concrete strength. This shows that weaker concrete can benefit from the effects of confinement, but for stronger concretes the effects are much less marked. If the objective is to maximise the energy dissipation by increasing the area under the stress-strain curve, then the use of a moderate concrete strength (≈ 40 MPa) is preferable to the use of very high strength concrete. The numerical results also showed that for high-strength concrete (> 60 MPa) the spirals did not reach their ultimate strength, with the concrete strength reducing to negligible values before the spiral snapped.

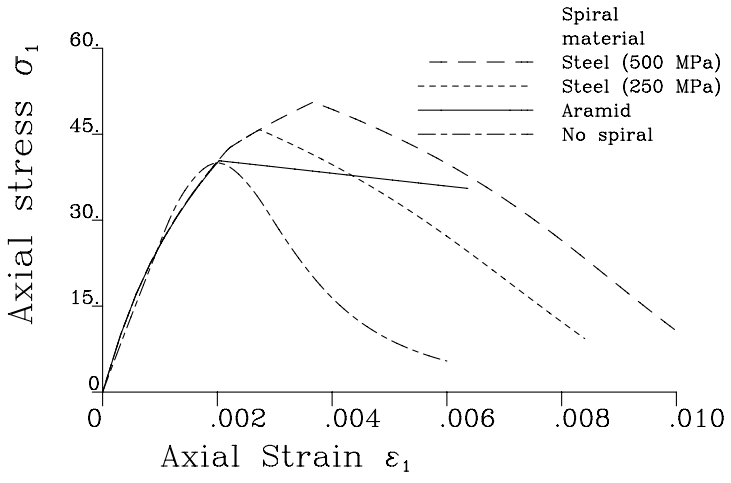

Fig. 6 Comparison between the use of aramid and steel spirals of different strength.

The effect of using steel for confinement is shown in Figure 6 for concrete with a strength of 40 MPa and a spiral pitch of 20 mm. Results are shown for steel with yield strengths of 250 and 500 MPa (Young's modulus 200 GPa and cross sectional area 5.3 mm^2). The additional stiffness of the steel increases the passive strength of the concrete above that of the aramid spirals, but when the steel yields no further enhancement of strength occurs and the applied stress drops rapidly.

4 CONCRETE WITH TWO INTERLOCKING SPIRALS

The analysis given above applies to axi-symmetric cylinders. For sections with overlapping spirals, the confining stresses σ_2 and σ_3 cannot be expressed as simple functions of the spiral strain and will also not be equal. Thus, the degree of confinement can be expected to vary and a method is required which allows the $\sigma_1 - \varepsilon_1$ curve to be obtained for the more realistic situation.

One possibility is to perform a global analysis of a beam using a finite element analysis that incorporates Kotsovos' model and also includes the spirals themselves as discrete elements. In general applications, however, it will not be sensible to perform a finite element analysis each time; instead, a method is sought which allows the effects of the interlock to be taken into account more easily.

Consider the case of concrete reinforced with two interlocking spirals. The concrete inside the overlapping area experiences a higher confining stress than that in the outer areas since it is under stress induced by both spirals simultaneously. If the uniform confining stress induced by a single spiral is σ_L, then the concrete inside the interlocking area must be subjected to a stress between σ_L and $2\sigma_L$. The concrete in the outer area might also be affected by the interlocking action but the variation can be expected to be significantly smaller.

If two interlocking spirals are placed inside a rectangular column, the cross section can be divided into three zones; a doubly-confined area, a singly-confined area and cover concrete (see Figure 7). Inside the doubly-confined area of concrete, the spacing of the spiral can be idealised as being half that of the singly-confined area, assuming the spirals have equal pitch. The lateral pressure on the inner boundary of the doubly-confined area is larger than that on the outer boundary of the singly-confined area. Tanaka [1] used the concept of the volumetric ratio of spirals and pointed out that the degree of confinement for the compression zone in the extremities of the core section confined by interlocking spirals may be less than that in the rest of the interlocking area. This is due to the uneven lateral pressure distribution that is generated. In order to take this into consideration, global *x*-*y* axes are defined and the coordinate system is applied to the layout of interlocking spirals (Figure 7). It is proposed that magnifying factors k should be used to allow for the variation in confining stress in the two areas. Separate factors will be used for singly-confined and doubly confined regions, with different factors for the *x*- and *y*-directions, giving a total of 4 factors. They take the form:-

$$\sigma_X^{sc} = \sigma_L \times k_X^{sc} \tag{3}$$

The values of k_X and k_Y largely depend upon the ratio of the centre-to-centre distance (c_{sp}) of the two interlocking spirals to the diameter of spiral (d_{sp}). Using the same pitch for the two spirals, the variations of the correction factor in two orthogonal directions in both the doubly-confined and singly-confined areas can be determined by means of a one-off finite element analysis.

The finite element analysis assumes that the concrete is linearly elastic and that each spiral induces a uniform inward pressure, which is equivalent to saying that the stress in the spirals is constant around the complete loop. The principal stresses induced at each node in the two confined zones are determined, but since the orientation of the principal directions vary over the section, the stresses in two fixed orthogonal directions are calculated. These are then averaged over the two regions to give the four values for the correction factor. These correction factors are then used to vary the lateral stresses applied in the actively confined analysis.

A notional lateral pressure of 100 units was assumed. The nodes along the axes of symmetry, and those along the spirals themselves, were specified and an automatic mesh generator then produced the rest of the nodes inside the spirals. Triangular elements were adopted throughout; typically about 1000 elements were used. The nodes along the axes of symmetry were restrained by roller support conditions to maintain symmetry (see Figure 8). A plane-strain linear-elastic material

was assumed since the object of the exercise was to determine the magnitudes of the principal stresses everywhere.

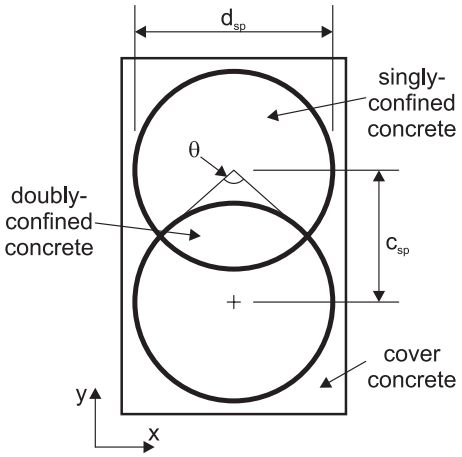

Fig. 7 Section with two interlocking spirals.

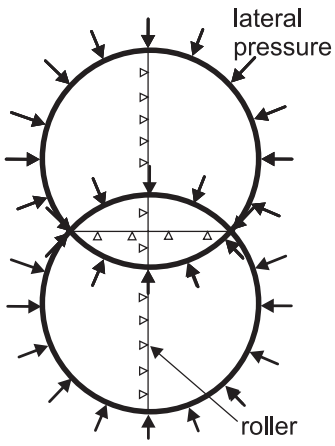

Fig. 8 Layout of finite element model.

In forming the best-fit equation, c_{sp}/d_{sp} is used as the parameter indicating the degree of overlapping of the spirals. A third order least-squares fitting is used, and the magnification factors for the singly-confined and doubly-confined portions of concrete in the two global directions were determined separately [2,20]. The results are plotted in Figure 9 for $0 < c_{sp}/d_{sp} < 1$. When $c_{sp}/d_{sp} = 0$, a complete overlap is formed and there is no singly-confined area. When $c_{sp}/d_{sp} = 1$, the two spirals touch each other and there is no doubly-confined region.

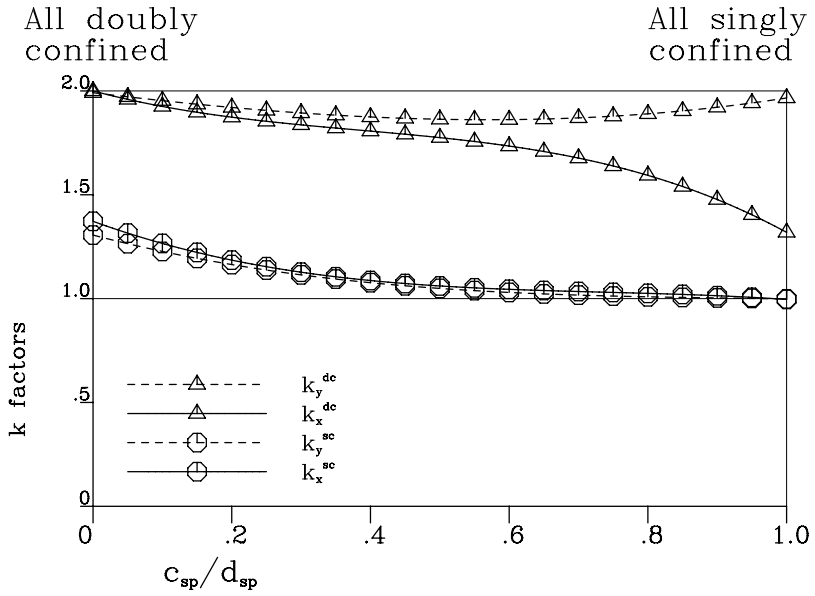

Fig. 9 Variation of magnification factors with degree of overlap of spirals.

The analysis then proceeds as before, using the appropriate k factors obtained from Figure 9; the revised values for the lateral stresses σ_2 and σ_3 are then used in the active analysis.

It must be stressed that in the analysis given here it is assumed that the strain in the spiral takes a constant average value, which is given by $\varepsilon_{sp} = \varepsilon_2$. This allows the assumption that the inward pressure from the spiral is uniform, and hence allows the use of the k factors determined from the finite element analysis. If this assumption is not made it would be necessary to perform detailed finite

element analyses to see how the spiral strain varied around the circle each time the method was applied, which would be both prohibitively expensive in computer time and unnecessary.

Figure 10 shows the passive confinement responses for a concrete with a strength of 40 MPa and aramid spirals with a pitch of 20 mm. The responses for the doubly-confined concrete with four different c_{sp}/d_{sp} values are shown. There is a small variation with this factor, but it is not significant. Also shown are the responses for singly reinforced concrete with spacing of 20 mm and 10 mm. The response for s = 10 mm is not the same as that for c_{sp}/d_{sp} = 0.0 because of the effect of the $(1-s/d_c)$ term; doubling the area of the spiral does not produce the same effect as halving the spacing due to the reduced confinement between the spirals.

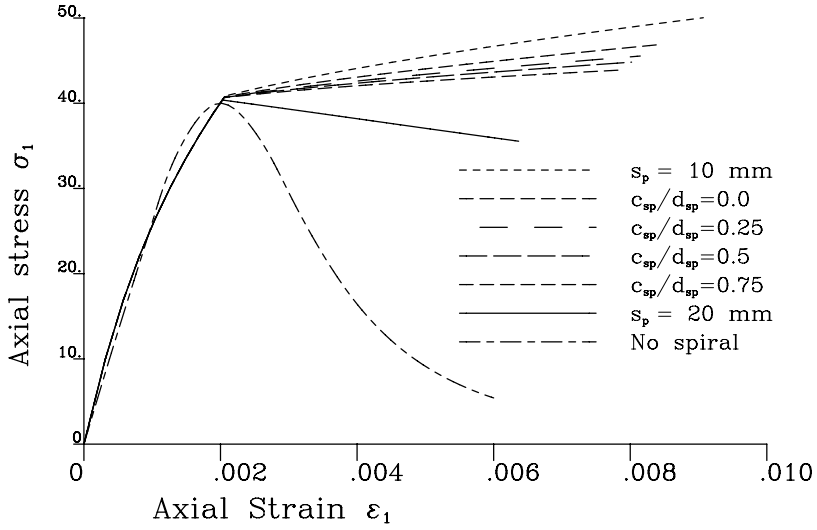

Fig. 10 Effect of degree of overlap on the behaviour of doubly-reinforced concrete.

When determining the overall load-extension response of an element containing all three types of concrete, the stress-strain curves for each element should be multiplied by the appropriate cross-sectional area. Due to the differences in the stress state of the singly-confined area and doubly-confined areas, the end-points of these stress-strain curves are different. It is postulated that the section reaches its failure state when the first spiral-snapping occurs, at which point the confinement ceases to be effective and the concrete becomes unconfined. Therefore, the smaller strain value of the two end-points gives the failure strain of the concrete with interlocked spirals (ε_{cc}^{u}) (Figure 11).

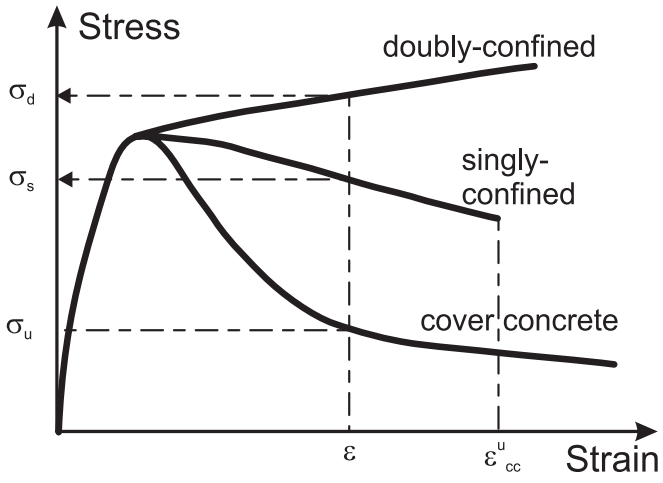

Fig. 11 Stress-strain curves for the three different areas.

5 ECCENTRIC ANALYSIS FOR CONCRETE WITH INTERLOCKING SPIRALS

The analysis so far has assumed that the external force is applied axially, so that the resulting force is aligned with the centre of the specimen and the axial strain is uniform across the section. However, if this analysis is to be applied to the compression zones of beams, the strain can be expected to vary across the section.

If it is assumed that the stress-strain curves for unconfined, singly-confined and doubly-confined concrete, as determined above, are still valid, then it is possible to use these to determine the force/moment versus axial strain/curvature relationships, as required.

For example, to determine the ultimate value of the axial force applied at a fixed eccentricity e, the position of the neutral axis of the section can be varied until the resulting force and moment match the required eccentricity. Failure is assumed to occur when the confined concrete reaches its ultimate strain (ε_{cc}^{u}). It is assumed that when concrete is subjected to a tensile strain, it cracks and carries no load. The procedure can be summarised as follows:

1. Determine the centre of pressure from the applied force and moment.
2. Assume a neutral axis depth, x.
3. The concrete section is then divided into small slices; each may contain three kinds of elements. By assuming that the ultimate strain of the confined concrete (ε_{cc}^{u}) is reached at the most confined edge, the strain at the middle of each element can be calculated.
4. The appropriate stress-strain model for both confined and unconfined areas is then used, from which the corresponding stress values are determined (Figure 12).
5. The axial force (N), moment (M) and corresponding centre of pressure are obtained by summing the effects of the elemental stress and the associated area.
6. If the centre of pressure does not match the desired value, the neutral axis depth is adjusted and the process repeated until a satisfactory value is obtained.
7. The curvature (κ) and axial strain at the centre of the rectangular block (ε_a) are then calculated.

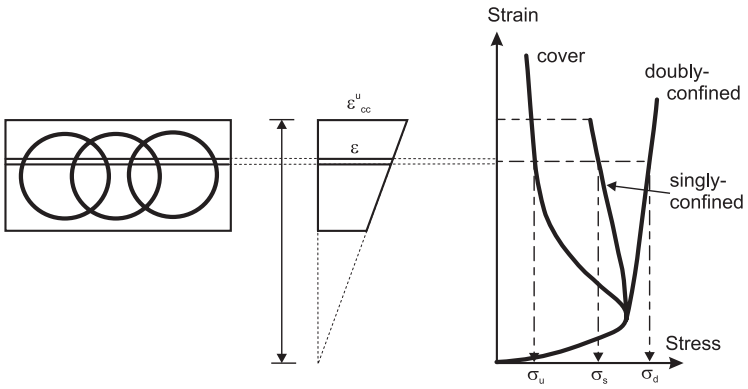

Fig. 12 Eccentric analysis of concrete with interlocking spirals.

It should be noted that this analysis requires that the strain in the spiral varies across the depth of the compression zone and takes the value it would have had if a uniaxial compressive strain of the appropriate value were applied to the section. This is not necessarily the case but is a reasonable assumption.

This procedure can be adapted easily to find other relationships; for example, to determine the moment-curvature relationship for a given location of the centre of pressure, the extreme fibre strain can be varied from zero up to the failure value assumed above.

6 CONCLUSIONS

It has been shown that Kotsovos' model for triaxially confined concrete can be used to determine the behaviour of concrete contained within passive spirals of reinforcement. This has been applied to cylinders reinforced with spirals of aramid fibres and the effects of varying both the spiral pitch and the concrete strength have been studied. High strength concrete does not benefit significantly from

confinement since it is stiffer and does not generate sufficient lateral expansion to mobilise the confining stress. The best effect of confinement (in terms of the energy dissipated) is obtained for concretes of moderate strength.

The differences associated with the use of steel reinforcement have been studied. Steel is more effective at providing confinement up to yield, due to the higher stiffness, but once the steel yields the strength drops off rapidly.

It has been shown that the area contained within the overlapping region of two spirals can be studied by the use of a finite element analysis. This allows the effect of the varying geometry on the confining stresses to be determined, which can then be used in the passive model to obtain different stress-strain curves for the singly-confined and doubly-confined regions.

Finally, it has been shown how the model can be used to determine the behaviour of confined concrete in the compression zone of beams where the strain varies through the depth.

ACKNOWLEDGEMENTS

The second author was supported in this work by the Croucher Foundation.

REFERENCES

[1] Tanaka H. and Park R. "Seismic design and behavior of reinforced concrete columns with interlocking spirals." *ACI Struct. J.*, 90, 192-203, 1993.

[2] Leung H.Y. . "Aramid fibre spirals to confine concrete in compression.", *PhD thesis*, University of Cambridge, UK., 200pp, 2000.

[3] Choi S., Thienel K.C. and Shah S.P. "Strain softening of concrete in compression under different end constraints." *Mag. Concr. Res.*, 48(175), 103-115, 1996.

[4] Hsu L.S. and Hsu C.T.T. "Complete stress-strain behaviour of high-strength concrete under compression." *Mag. Concr. Res.*, 46(169), 301-312, 1994.

[5] Imran I. and Pantazopoulou S.J. "Experimental study of plain concrete under triaxial stress." *ACI Mater. J.*, 93, 589-601, 1996.

[6] Kotsovos M.D. and Pavlovic M.N. *Structural Concrete*, Thomas Telford, London, 1995.

[7] Lahlou K., Aitchin P.C. and Chaallal O. "Behaviour of high-strength concrete under confined stresses." *Cement & Concrete Composites*, 14, 185-193, 1992.

[8] Mansur M.A., Wee T.H. and Chin M.S. "Derivation of the complete stress-strain curves for concrete in compression." *Mag. Concr. Res.*, 47(173), 285-290, 1995.

[9] Morales S.M., Nilson A.H. and Slate F.O. "Spirally-reinforced high-strength concrete columns." *Report No.82-10*, Cornell University, 255pp, 1982.

[10] Kotsovos M.D. and Newman J.B. "Behavior of concrete under multiaxial stress." *ACI J.*, 74, 443-446, 1977.

[11] Kotsovos M.D. "Consideration of triaxial stress conditions in design: A necessity." *ACI Struct. J.*, 84, 266-273, 1987.

[12] Kotsovos M.D. and Pavlovic M.N. *Ultimate limit-state design of concrete structures: A new approach*, Thomas Telford, London, 1999.

[13] Mander J.B., Priestley M.J.N. and Park R. "Theoretical stress-strain behavior of confined concrete." *ASCE J. Struct. Engng.,* 114(8), 1804-1826, 1988.

[14] Mander J.B., Priestley M.J.N. and Park R. "Observed stress-strain behavior of confined concrete." *ASCE J. Struct. Engng.*, 114(8), 1827-1849, 1988.

[15] Mander J.B., Priestley M.J.N. and Park R. *ASCE J. Struct. Engng.*, 117(2),.628-629, 1991.

[16] Richart F.E., Brandtzaeg A. and Brown R.L. "A study of the failure of concrete under combined compressive stresses." *University of Illinois Engineering Experiment Station Bulletin*, 185, 1928.

[17] Saadatmanesh H., Ehsani M.R. and Li M.W. "Strength and ductility of concrete columns externally reinforced with fiber composite straps.", *ACI Struct. J.*, 91, 434-447, 1994.

[18] Kotsovos M.D. and Newman J.B. "A mathematical description of the deformational behaviour of concrete under complex loading." *Mag. Concr. Res.*, 31(107), 77-90, 1979.

[19] Kotsovos M.D. and Newman J.B. (1980). "Mathematical description of deformational behavior of concrete under generalized stress beyond ultimate strength." *ACI J.*, 77, 340-346.

[20] Leung H.Y. and Burgoyne C.J., "The uniaxial stress-strain relationship of spirally-confined concrete", *Materials Journal American Concrete Institute*, 102/6, 445-453, November 2005.

[21] Carreira D.J. and Chu K.H. "Stress-strain relationship for plain concrete in compression." *ACI J.*, 82, 797-804, 1985.